◆ Human Brain Mapping 34:1415–1426 (2013) ◆

Adaptive Changes in the Neuromagnetic Response of the Primary and Association Somatosensory Areas Following Repetitive Tactile Hand Stimulation in Humans

Elena Anda Popescu,[1] Steven M. Barlow,[2,3] Lalit Venkatesan,[3] Jingyan Wang,[2] and Mihai Popescu[1,4]*

[1]*Hoglund Brain Imaging Center, The University of Kansas Medical Center, Kansas City, Kansas*
[2]*Department of Speech, Language and Hearing, The University of Kansas, Lawrence, Kansas*
[3]*Intercampus Program in Neuroscience, The University of Kansas, Lawrence, Kansas*
[4]*Department of Molecular and Integrative Physiology, The University of Kansas Medical Center, Kansas City, Kansas*

Abstract: Cortical adaptation in the primary somatosensory cortex (SI) has been probed using different stimulation modalities and recording techniques, in both human and animal studies. In contrast, considerably less knowledge has been gained about the adaptation profiles in other areas of the cortical somatosensory network. Using magnetoencephalography (MEG), we examined the patterns of short-term adaptation for evoked responses in SI and somatosensory association areas during tactile stimulation applied to the glabrous skin of the hand. Cutaneous stimuli were delivered as trains of serial pulses with a constant frequency of 2 Hz and 4 Hz in separate runs, and a constant inter-train interval of 5 s. The unilateral stimuli elicited transient responses to the serial pulses in the train, with several response components that were separated by independent component analysis. Subsequent source reconstruction techniques identified regional generators in the contralateral SI and somatosensory association areas in the posterior parietal cortex (PPC). Activity in the bilateral secondary somatosensory cortex (i.e., SII/PV) was also identified, although less consistently across subjects. The dynamics of the evoked activity in each area and the frequency-dependent adaptation effects were assessed from the changes in the relative amplitude of serial responses in each train. We show that the adaptation profiles in SI and PPC areas can be quantitatively characterized from neuromagnetic recordings using tactile stimulation, with the sensitivity to repetitive stimulation increasing from SI to PPC. A similar approach for SII/PV has proven less straightforward, potentially due to the tendency of these areas to respond selectively to certain stimuli. *Hum Brain Mapp 34:1415–1426, 2013.* © 2012 Wiley Periodicals, Inc.

Key words: cortical adaptation; primary somatosensory cortex; somatosensory association areas; tactile stimulation; magnetoencephalography (MEG)

Contract grant sponsor: National Institutes of Health (NIH); Contract grant numbers: R01 DC003311, P30 HD02528, P30 DC005803, HD002528; Contract grant sponsor: Department of Health and Human Services; Contract grant numbers: HF15011, HF00201. Contract grant sponsors: Sutherland Foundation; Forrest and Sally Hoglund.

*Correspondence to: Mihai Popescu, Hoglund Brain Imaging Center, The University of Kansas Medical Center, MS 1052, 3901 Rainbow Boulevard, Kansas City, KS 66160.
E-mail: mpopescu@kumc.edu

Received for publication 21 April 2011; Revised 7 September 2011; Accepted 25 October 2011

DOI: 10.1002/hbm.21519

Published online 14 February 2012 in Wiley Online Library (wileyonlinelibrary.com).

INTRODUCTION

Early studies in humans [Gescheider and Wright, 1969; Hahn, 1966; Lundstrom, 1986] showed that adaptation to somatosensory inputs is reflected by reduced subjective intensity and elevation of the detection thresholds for subsequent stimuli. Additional evidence indicated that sustained somatosensory inputs generate a transition from a nonadapted state that facilitates the detection of the stimulus and its salient features to an adapted state that enhances the discrimination of its fine characteristics [Goble and Hollins, 1993, 1994; Tommerdahl et al., 2005]. Such psychophysical observations are consistent with findings from electrophysiological and optical imaging studies of neuronal response adaptation at multiple levels of organization in the primary somatosensory cortex (SI). Sustained sensory stimulation triggers changes in the spiking activity of middle-layer cortical neurons that indicate a switch in their role from coincidence detectors (optimally tuned for stimulus detection) in the nonadapted state to integrators (tuned for stimulus discrimination) following adaptation [Wang et al., 2010]. These adaptive changes observed at the single-cell level are accompanied by changes in the activity of local cortical neuronal populations [Gabernet et al., 2005; Heiss et al., 2008; Higley and Contreras, 2006]. The afferent input from a localized tactile stimulus evokes an initial activity within a relatively extended area in SI, driving excitatory responses in a large number of neurons that respond to many different tactile stimuli [Frostig et al., 2008; Whitsel et al., 1989]. With sustained stimulation, a dynamic cortical inhibitory mechanism determines a rapid reorganization of the initially extended SI activation into a reproducible pattern of activity consisting of complex arrays of columnar aggregates with higher sensitivity and specificity (tuning) for the attributes of the repetitive stimulus [Tommerdahl and Whitsel, 1996; Whitsel et al., 1989, 1991]. These changes result in a decrease in the overall SI activity with sustained stimulation, which can be investigated in humans using noninvasive, high-temporal resolution electroencephalography (EEG) or magnetoencephalography (MEG) recordings.

Although it is acknowledged that adaptation plays an important role in sensory function, it remains largely unknown if/how adaptive changes at multiple hierarchical levels of the cortical somatosensory network (i.e., within and beyond SI) contribute to the changes in behavioral performance observed with sustained sensory inputs. This cortical network includes multiple somatic areas that bound SI, which were collectively identified as somatosensory association areas [Caselli, 1993], i.e., secondary somatosensory (SII) and parietal ventral (PV) areas located ventro-lateral to SI in the parietal operculum, and somatosensory association areas corresponding to Brodmann's areas 7 and 5 located dorso-lateral and dorso-medial to SI, respectively. In the absence of specific neuroanatomical information, the ventral areas are considered jointly as SII/PV, whereas the dorsal areas are commonly referred to as somatosensory association areas in the posterior parietal cortex (PPC). It was shown that SII/PV and PPC somatosensory association areas have different anatomical connections and neurophysiological properties [Caselli, 1993; Hsiao, 2008]. Somatosensory inputs can reach these association areas not only via thalamo-cortical connections but through cortico-cortical connections from SI and from other association areas as well [Cavada and Goldman-Rakic, 1989a,b; Pons et al., 1992].

Early EEG studies of cortical somatosensory adaptation examined the changes in the evoked response amplitude during repetitive stimulation [for review, see McLaughlin and Kelly, 1993], but limitations in the existing methodology did not allow to estimate accurately the multiple sources of the cortical somatosensory network. Subsequent MEG studies using electrical stimulation and source reconstruction techniques showed sequential cortical activity in distinct areas of the cortical somatosensory network, that is, in SI and SII/PV [e.g., Hamada and Suzuki, 2005; Hari et al., 1990, 1993; Mauguière et al., 1997], and additionally in PPC [Forss et al., 1994a, 1999; Hari and Forss, 1999], without focusing on the changes in the evoked activity with sustained stimulation. Other MEG studies examined directly the cortical adaptation in SI and SII using trains of electrical stimuli [Hamada et al., 2002; Ou et al., 2009]. Electrical stimulation, however, bypasses the sensory skin receptors and entrains undifferentiated afferents and motor efferent fibers, altering the adaptation mechanisms at subcortical and cortical levels due to abnormal lateral inhibition [Willis and Coggeshall, 1991]. The potential advantages of using tactile stimuli that activate a relatively homogenous population of mechanoreceptors corresponding to a local definite skin area were widely acknowledged [Franzén and Offenloch, 1969; Hashimoto et al., 1990; Pratt et al., 1980]. However, only a few recent MEG studies used tactile stimulation paradigms to characterize cortical somatosensory adaptation, and they focused exclusively on the early response components corresponding to SI activity [Nangini et al., 2009; Popescu et al., 2010; Renvall et al., 2005].

The specific aim of our study was to assess the effectiveness of spatiotemporal data analysis using independent component analysis (ICA) and magnetic source imaging for characterizing region-specific adaptation induced by sustained tactile stimulation in distinct areas of the cortical somatosensory network. If effective, such an approach can support future studies investigating if/how the adaptive changes at multiple levels of the cortical somatosensory network contribute to changes in behavioral performance, or their correlation with an abnormal sensory perception in specific neurological conditions. For this purpose, we recorded neuromagnetic somatosensory evoked fields (SEFs) in response to trains of tactile pulses delivered to the glabrous skin of the hand at different stimulation frequencies. Our results indicate that the primary somatosensory cortex and somatosensory association areas exhibit varying levels of adaptation, with the sensitivity to repetitive stimulation increasing from SI to PPC and SII/PV

areas. We show that a quantitative characterization of the adaptation profiles in PPC can be obtained using tactile stimulation paradigms for the range of stimulation frequencies used in our study, but a similar approach for SII/PV areas has proven less straightforward. These findings are discussed by highlighting the selective nature of these somatosensory association areas in relation to their functional role and tendency to respond predominantly to certain stimuli [Young et al., 2004].

METHODS

Subjects, Stimuli, and Data Acquisition

Somatosensory evoked fields were recorded from 10 female subjects (mean age: 24 years, 10 months ± 2 years, 11 months) without known neurological conditions, who agreed to participate in a larger study examining the neuromagnetic responses to patterned cutaneous stimuli delivered using a novel pneumatic tactile stimulator [Venkatesan et al., 2010]. All participants were right-handed according to the Edinburgh Handedness Inventory [Oldfield, 1971]. Informed consent was obtained from each subject before participation in the experiment. The study was approved by the Institutional Review Board of the University of Kansas Medical Center. One subject was excluded from further analysis due to low signal-to-noise ratio in one experimental condition. The data presented in this report pertain to the remaining group of 9 subjects.

The tactile stimuli were delivered using a servo-controlled pneumatic amplifier. A silicone tube (4.6 m length, 3.2 mm internal diameter, 1.6 mm wall thickness) was used to conduct the pneumatic pulse stimuli from the servo motor to a small-bore pneumatic actuator (TAC-Cell) attached with double-adhesive tape collars on the glabrous skin of the right hand, over the distal phalanges and close to the interphalangeal articulations of the index and middle fingers that remained relaxed in a resting position. The potential advantages of the simultaneous stimulation of the two adjacent fingers are: (1) stimulation of a larger skin area activates a larger cortical area in SI, and typically results in a higher signal-to-noise ratio, and (2) spatially extended stimuli presumably engage more efficiently the somatosensory association areas characterized by larger receptive fields. The TAC-Cell used in our study was a 5 ml round vial with a polyethylene cap, designed to create an internal lumen with a diameter of 19.3 mm. Pneumatic charging (+125 cm H_2O) generates a deflection of the 0.13 mm silicone membrane that is secured between the vial rim and snap-type cap, applying a light pressure stimulus to the skin surface with each deflection. The membrane displacement had a rise-time of 27 ms (defined as the time interval between the 10% and 90% of the maximum displacement) and a duration of 50 ms (measured between the half-maximum displacement on the rising and falling slopes of the pressure wave). All latencies reported in this study are corrected for a 17 ms mechanical response delay between the trigger to the pneumatic servo and the onset of the membrane deflection.

The stimulation session consisted of three successive runs with 6-pulse trains of stimuli delivered in blocks of 125 trials in each run. The frequency of the tactile pulses in each train was constant during the run and set to 2 Hz, 4 Hz, and 8 Hz, respectively. The pulse duration (50 ms) and inter-trial interval (5 s, measured from the last stimulus in a train to the first stimulus in the next train) were constant across all runs. The order of the runs was randomized across subjects.

MEG signals were recorded in a magnetically shielded room using a whole-head CTF 151-channel system with axial gradiometers sensors (5 cm baseline). Two bipolar (vertical and horizontal) EOG channels were simultaneously recorded to identify the trials affected by eye movement or blinks artifacts. The head position relative to the sensor array was determined by feeding current into three localization coils placed at nasion and left- and right-preauricular points, respectively. The data were recorded in continuous mode using a sampling rate of 600 Hz and a pass-band of 0–150 Hz. Magnetic resonance imaging (T_1-weighted scans) were performed for all participants immediately after the MEG experiment using registration landmarks placed at the localization coils positions.

MEG Data Analysis

Data Pre-Processing

The recorded MEG signals were band-pass filtered between 1.5 Hz and 50 Hz using bidirectional fourth-order Butterworth filters, to remove the sustained fields that occurred during the stimulus trains and to facilitate the identification of the transient response components. Epochs starting 1.0 s before the first pulse and ending 1.0 s after the last pulse in each trial were visually inspected to discard trials with eye movement or other artifacts. The remaining artifact-free trials (not less than 90 for each subject and condition) were averaged separately for each run and the DC was offset using the prestimulus period as a baseline.

Strong suppression of the transient evoked responses to the second and subsequent pulses in the train was observed at the 8 Hz stimulation rate for both early and late response components. In particular, for the response components later shown to be generated by the activity in the somatosensory association areas, that is, PPC and SII/PV, the strong suppression hindered the reliable identification of these subsequent transient evoked responses. Therefore, a quantitative comparison between the adaptive changes in SI versus any of the somatosensory association areas was not possible for the 8 Hz stimulation rate, and the analysis reported in this study is limited to the 2 Hz and 4 Hz stimulation conditions.

Aiming to provide an efficient practical approach for the source estimation of the multiple component response, the

averaged datasets for each subject and condition were first decomposed using a PCA-filtering ICA algorithm [Hyvärinen and Oja, 2000]. PCA-filtering was applied to reduce the data dimensionality, such that an appropriate statistical measure of independence could be achieved by the subsequent ICA, which was used to segregate the contribution of each independent component (IC) to the overall magnetic field. The number of components was determined for each dataset based on a significant decrease in the singular values of the spatio-temporal data matrix, resulting in 3 or 4 ICs per dataset across subjects and conditions.

Source Reconstruction

For each dataset, the source reconstruction was performed separately for each IC in CURRY (Neuroscan, Compumedics), using a spherically symmetric volume conductor model fitted to the skull (segmented from the MRI data). The source space was defined as a regular grid of points in the brain volume (average distance between points was 3 mm). Because the independence constraint in ICA relies entirely on the amplitude distribution of the sensor data and does not include assumptions about the underlying sources, each IC can reflect the activity of single or multiple synchronous neuronal generators [Delorme and Makeig, 2004; Hironaga and Ioannides, 2007; Vigário et al., 2000]. Accordingly, the ICs of interest were localized using a two-step source reconstruction algorithm. First, a current density analysis using sLORETA [Pascual-Marqui, 2002] was performed to verify if single or multiple regional generators account for each IC and to identify the corresponding spatial peaks of activity. sLORETA uses the standardization of a minimum norm inverse solution, and does not require a priori information about the number of active sources. Second, a location constrained dipole analysis (with the positions of the dipoles at the spatial peaks of activity retrieved by sLORETA) was performed to obtain estimates of the direction and strength for each active brain region. The dipole fitting procedure allowed characterizing the source strengths using current units rather than the statistical measures retrieved by sLORETA.

Statistical Analysis

Analyses of variance (ANOVA) with dipole locations, peak strengths, and peak latencies as dependent variables were performed in STATVIEW 5 (SAS Institute), with explicit comparisons between response components and stimulation rates.

RESULTS

Neuromagnetic SEFs to Pulse Trains of Tactile Stimuli

Figure 1 exemplifies the averaged SEF data for the 2 Hz stimulation condition. Each pulse stimulus in the train produced transient neuromagnetic responses with a time-varying morphology indicating the existence of multiple SEF sources peaking at different latencies. The first component of the response (marked with a vertical line in Fig. 1b) peaks in this example at 74 ms, whereas the second component peaks at 104 ms. Each of these two components is characterized by a unilateral, distinctly dipolar pattern of the magnetic field (Fig. 1c), confined to a different subarray of sensors in the left hemisphere (contralateral to the stimulation site). These two components are followed by a third component peaking at 131 ms, which is characterized by a bilateral dipolar pattern of the magnetic field that suggests bilateral activity evoked in SII/PV areas, as previously shown by other MEG studies, most of them using electrical stimulation paradigms [Forss et al., 1994a,b, 1999; Hamada et al., 2002; Hari and Forss, 1999; Hari et al., 1990, 1993; Schnitzler et al., 1999; Zhu et al., 2007]. The dipolar pattern at the peak of the third component is asymmetric over the subarray of sensors covering each hemisphere (e.g., the negative magnetic field recorded by the posterior lateral sensors in the left hemisphere is higher than the positive magnetic field in left anterior lateral sensors). This can be partly due to the fact that the activity of the main generator of the second component (peaking at 104 ms) overlaps in time with the activity of these later bilateral sources. This is also suggested by the morphology of the sensor signals shown in Figure 1b, and by the way, it is reflected in the mean global field (MGF) trace, with the third component seen as a shoulder on the descending part of the most prominent (i.e., second) component. Subsequent pulses within the train evoke similar SEFs, although with different relative amplitudes of the components. Two observations regarding the inter-subject variability in the SEF responses at the sensors are worth mentioning. First, visual inspection of the two leading response components evoked by the first pulse in the train (i.e., without considering the effect of their short-adaptation patterns induced by the subsequent serial pulses) indicated that their relative amplitude was different between subjects, with the amplitude of the first component higher compared to the second component in some subjects, and lower in others. In addition, it was observed that the first 2 prominent components were followed by a series of other late response components (including the bilateral third component described above), with a markedly high inter-subject variability in latency and magnetic field topography (i.e., the sequence and/or characteristics of these late response components were not consistent across subjects). Similar response components of the averaged SEF data were obtained for the 4 Hz stimulation frequency (Fig. 3a,b).

Spatio-Temporal Reconstruction of the Independent Component Activity

The criteria used to determine how the ICs are related to the evoked response components peaking at different latencies were based on the visual inspection of the sensor

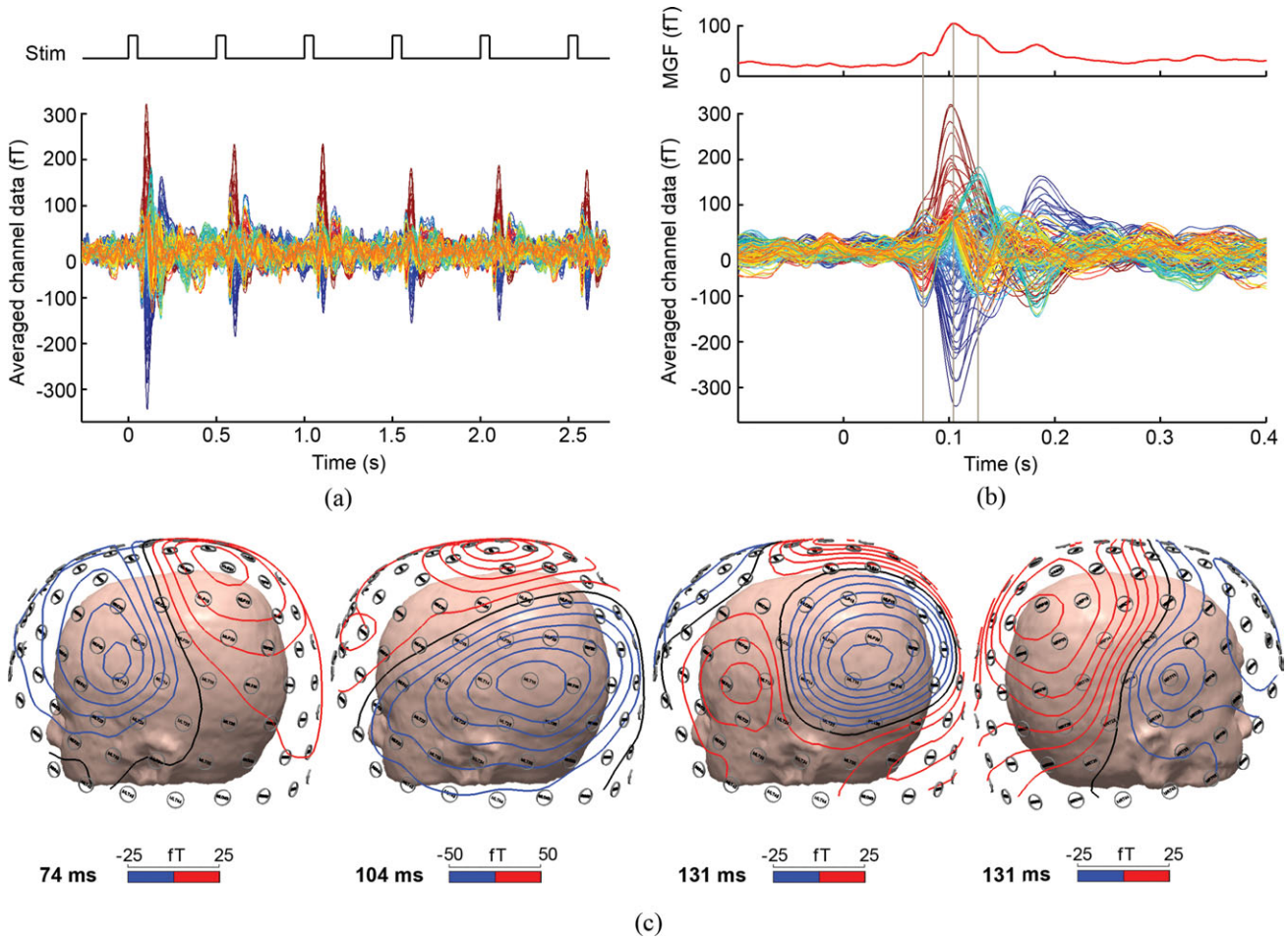

Figure 1.

(**a**) An illustration of the averaged neuromagnetic response evoked by 2 Hz stimulus trains is shown for one representative subject. (**b**) The response to the first pulse in the train is shown expanded for better visualization of the individual response components. The single red trace at the top displays the MGF computed across the whole channel array. (**c**) The magnetic field maps are shown at the peak latencies for the first 3 response components marked with vertical lines in panel (b) (fT values on color bars indicate the increment in isofield contour lines; black contour line corresponds to zero magnetic field). The first 2 components are characterized by dipolar magnetic field patterns confined to the contralateral (left) hemisphere; the third component is characterized by a bilateral magnetic field distribution (shown in left and right views). [Color figure can be viewed in the online issue, which is available at wileyonlinelibrary.com.]

map and temporal course of each IC. An example of three-component ICA decomposition is illustrated in Figure 2. The ICs (displayed in decreasing order of their data variance) have distinct spatial patterns of magnetic field (Fig. 2a) and temporal courses of activity (Fig. 2b). In this case, the associated magnetic field topography of each component is consistent with contralateral (IC1 and IC2) and bilateral (IC3) generators. The filtered MGF for each of these ICs (i.e., computed from the reconstructed sensor data reflecting the separate contribution of the corresponding IC) shown in Figure 2c matches closely the MGF of the averaged data at the peak latency of the corresponding evoked response component marked by vertical lines in Figure 1b (note that the first IC corresponds to the response component peaking at 104 ms). Later, including bilateral, response components and their corresponding ICs were heterogeneous across subjects, consistent with our observations about the morphology of the averaged evoked responses. Thus, for the purpose of our current study, only the ICs that segregated the response components around 70 ms (IC2 in Fig. 2b) and about 30 ms later (IC1 in Fig. 2b) were examined, as they represented the most consistent response components separated by the PCA-ICA algorithm and clearly identified for both stimulation conditions in 8 (out of 9) subjects that were included in the subsequent quantitative analysis. For these subjects,

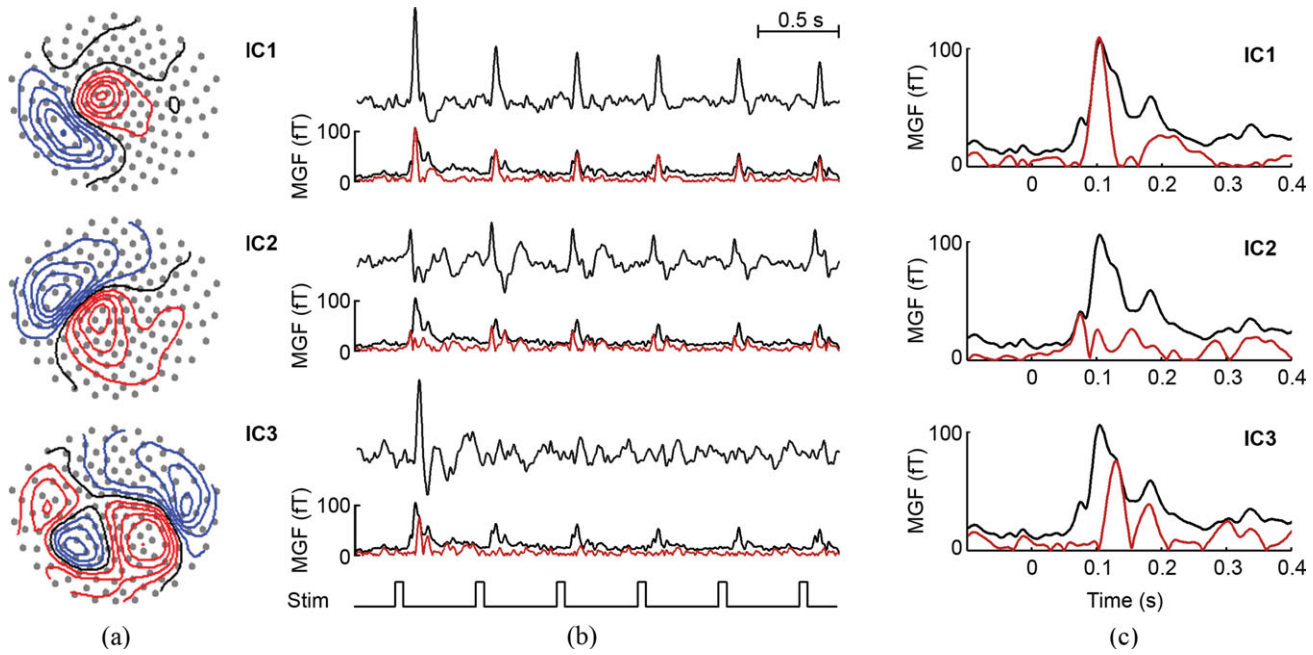

Figure 2.

(**a**) Interpolated magnetic isofield contours are shown for the three ICs (in decreasing order of their data variance) of the neuromagnetic response evoked by 2 Hz stimulus trains seen in Figure 1a. (**b**) The traces display the timecourse of activity corresponding to each IC, and contrast the filtered MGF (in red) against the MGF of the original data (in black) for each IC. (**c**) The filtered MGF (in red) is compared with the MGF of the original data (in black) for the duration of the first evoked response (expanded for better visualization); MGF is computed across the whole channel array. [Color figure can be viewed in the online issue, which is available at wileyonlinelibrary.com.]

similar ICA decompositions were obtained for the 2 Hz and 4 Hz stimulation rates, up to the order of ICs. Because ICs are sorted in decreasing order of their data variance, IC ranks are determined by the relative amplitude of the response components and by their frequency-dependent level of adaptation (the IC ordering does not represent an issue per se, as long as a direct correspondence between each IC and the response component it accounts for can be reliably determined). An example of ICA decomposition for the 4 Hz data (from the same subject as in Fig. 2b) is shown in Figure 3c. The time courses of the first 2 ICs exhibit clear transient responses after the onset of each pulse of stimulation, accounting accurately for the two early SEF peaks. Noteworthy, the ICs segregating these early response components show also subsequent activations at later latencies after each pulse (Figs. 2b and 3c), contributing to some of the late components that were observed in the averaged sensor data. In contrast, IC3 that segregates the contribution of the bilateral generators shows a clear response to the first stimulus in the train, but subsequent responses to the following stimuli have markedly reduced amplitude. The strong suppression of the late bilateral responses to the second and following pulses in the train was present for both stimulation rates in all subjects with a clearly identifiable bilateral component, that is, 5 out of the 9 subjects. PCA-ICA algorithm did not separate the late bilateral response components into ipsilateral and contralateral ICs (due to their temporal correlation). Therefore, the attenuation of these components with the serial position revealed a similar behavior for the ipsilateral and contralateral evoked responses. Moreover, the very small amplitude of these responses to subsequent stimuli hindered their reliable detection and the quantitative characterization of their adaptation profiles.

sLORETA source estimates for the IC peaking at ~70 ms after the onset of each stimulus retrieved maximal activity in the contralateral (left) central sulcus, indicating neuronal generators in the hand area of the primary somatosensory cortex (Fig. 4a). This is consistent with other MEG studies using tactile stimulation of the fingers [e.g., Forss et al., 1994a; Jones et al., 2007; Kakigi et al., 2000]. sLORETA estimates for the IC peaking at ~100 ms recovered maximal activity in the contralateral (left) posterior parietal cortex, in the posterior wall of the postcentral sulcus (Fig. 4b), which indicates neuronal generators in the dorsal somatosensory association areas in PPC, as previously reported using air-puff stimulation of the fingers [Forss et al., 1994b].

The results of the second step of source reconstruction (i.e., sLORETA-constrained dipole fitting) are exemplified in Figure 5 on T_1-weighted MRI orthogonal images. For the early (first) response component, dipoles were localized in the anterior wall of the postcentral gyrus, consistent with

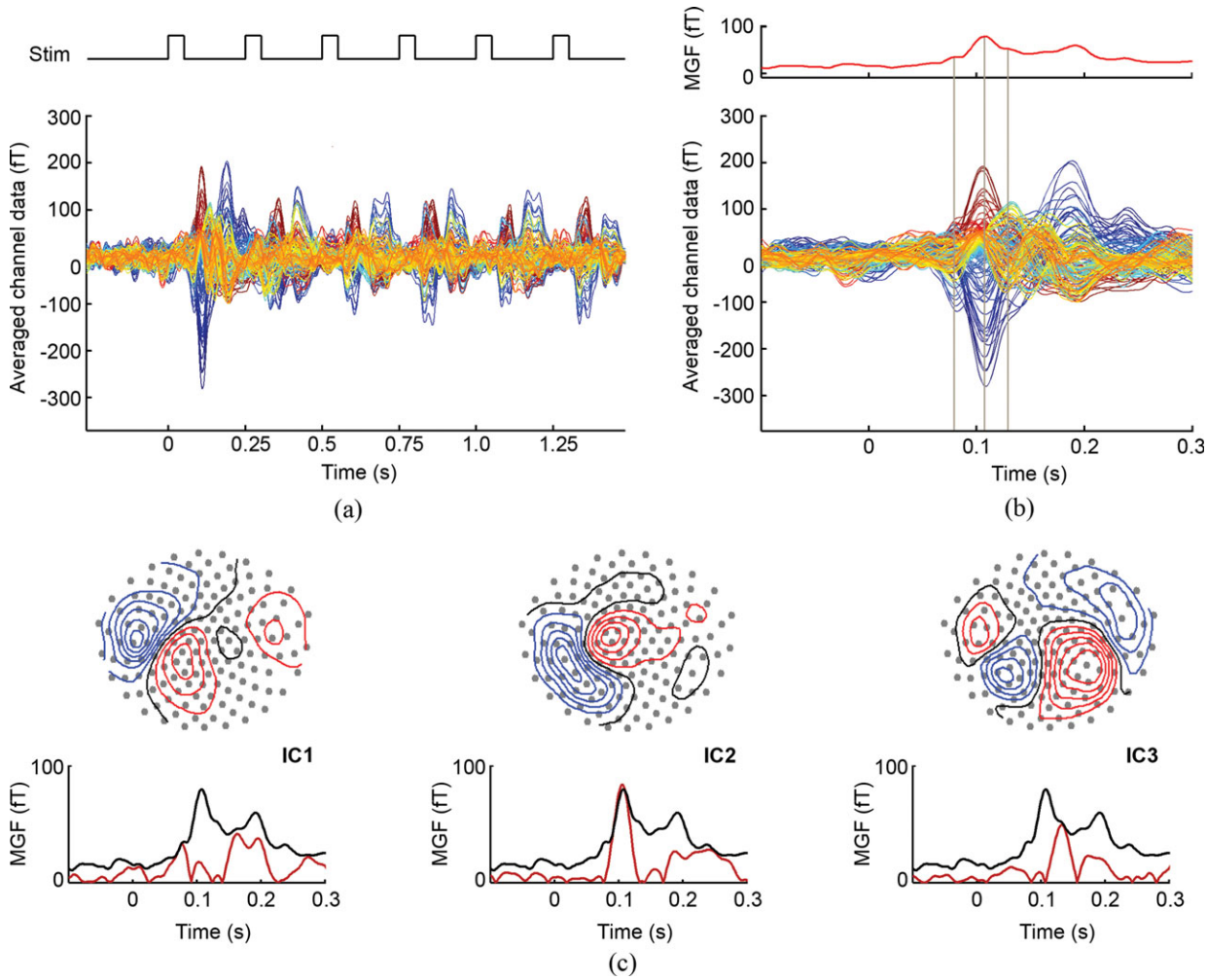

Figure 3.

(**a**) The averaged neuromagnetic response evoked by the 4 Hz stimulus trains is exemplified for the same subject shown in Figure 1. (**b**) The response to the first pulse in the train is shown expanded for better visualization of the response components. (**c**) The top panels show the interpolated magnetic isofield contours for the three ICs (in decreasing order of their data variance) corresponding to the neuromagnetic response shown in panel (a). The bottom panels display the filtered MGF (in red) compared with the MGF of the original data (in black) for the duration of the first evoked response. [Color figure can be viewed in the online issue, which is available at wileyonlinelibrary.com.]

generators in the proximal neuronal populations of SI areas 3b and 1. Dipoles for the second response component were localized in regions of the post-central sulcus, posterior, and slightly medial with respect to the SI source.

Source Locations

Because of the proximity of the generators for the two response components under study, we first analyzed their relative locations to verify consistency across subjects and conditions. Two-way repeated measures ANOVAs with response component (first and second with respect to peak latency) and stimulation rate (2 Hz and 4 Hz) as factors were performed separately for each of the three Cartesian coordinates (i.e., x, y, and z, as dependent variables) describing the dipole source locations across subjects and conditions for each of the two response components. This analysis showed significant main effects of response component for the Cartesian coordinates x (medio-lateral direction, $F = 7.66$, $P = 0.028$), y (posterior-anterior direction, $F = 12.58$, $P = 0.009$), and z (pointing toward the vertex, $F = 8.78$, $P = 0.021$). As no significant main effect of stimulation rate was detected (indicating no systematic difference in source locations with the stimulation rate), the source coordinates for each of the two stimulation rates were aggregated into a mean value for each subject. The averaged source positions across all subjects are summarized in Table I.

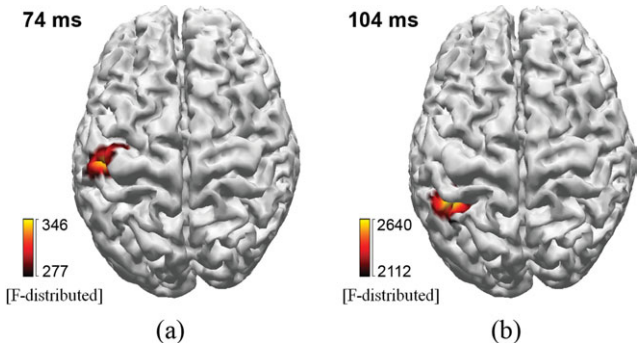

Figure 4.

The results of source estimation (i.e., current density reconstruction using sLORETA) are shown for each of the ICs that correspond to SI (**a**) and PPC (**b**) SEF response components. The activity maps are shown on the cortical surface at the peak latency of the first pulse in the train (for 2 Hz stimulation frequency), clipped at 80% of the spatial maximum for each source. [Color figure can be viewed in the online issue, which is available at wileyonlinelibrary.com.]

The results of this analysis showed a significantly different localization of the second component (peaking at ~100 ms) relative to the first component (SI, peaking at ~70 ms), that is, the source location of the second response component was more medial (mean $\Delta x = 5$ mm, SD = 5 mm), more posterior ($\Delta y = -9$ mm, SD = 7 mm), and more superior ($\Delta z = 6$ mm, SD = 6 mm), consistent with neuronal generators in the dorsal somatosensory association areas in PPC. The mean (across subjects) Euclidian distance between the two sources was 15 mm (SD = 7 mm).

Response Latencies

To test for the presence of stimulation rate- and brain area-dependent adaptation effects on the response latency, a three-way repeated measures ANOVA was performed, with stimulation rate (2 Hz vs. 4 Hz), brain area (SI vs. PPC), and serial position of the pulses in the train as independent variables, and the latency of the responses to stimuli (SEFs) as dependent variable. The test indicated a significant main effect of brain area ($F = 51.6$, $P = 0.0002$), and no significant effect of stimulation rate and no significant interactions. Thus, we observed no rate-specific or serial position-specific adaptation effects on the SI or PPC response latencies. Based on these observations, an aggregate value for the latency of each of the two response components was obtained for each subject by averaging across stimulation rates and pulses, and the subsequently estimated mean global values across subjects are summarized in Table I. The mean delay between the peak activity of the cortical response evoked in PPC versus SI was 29 ± 6 ms.

Response Amplitudes

Individual differences in the absolute response amplitude for the SI and PPC sources, which can be related to neuroanatomical differences or to physical factors, such as subject variability in the orientation of current sources relative to local radial direction, were eliminated by normalizing each source strength with the amplitude of the corresponding first response in the train for each subject in each stimulation condition. Figure 6 shows the mean normalized peak amplitudes as a function of serial position within the pulse train, for the two stimulation rates

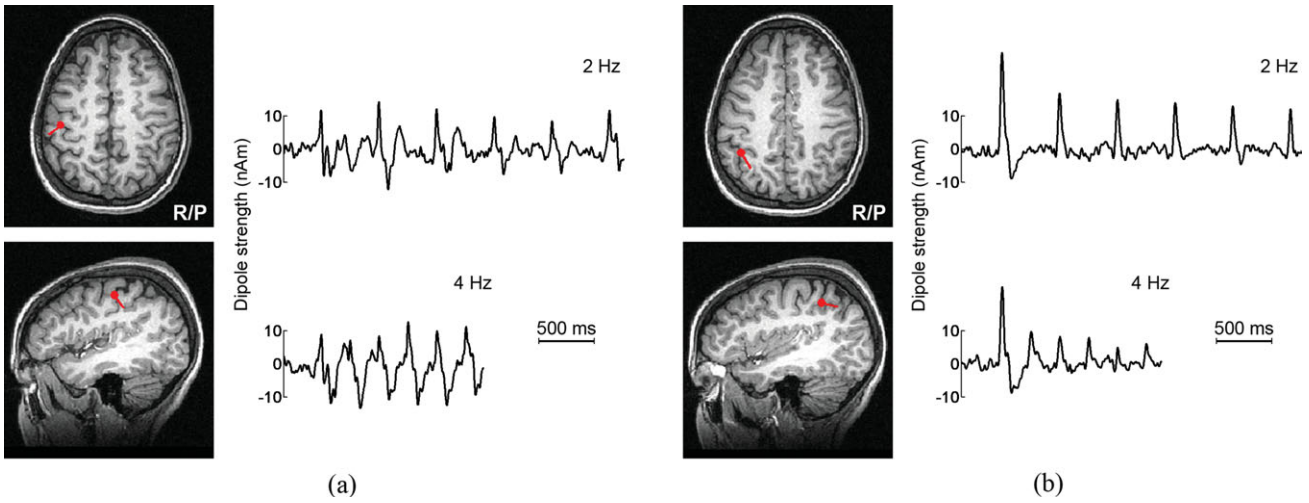

Figure 5.

Dipole locations and orientations (at the corresponding peak latencies) are shown in orthogonal axial and sagittal MRI slices for the SI (**a**) and PPC (**b**) generators. The dipole activation time-courses are displayed in adjacent panels for the 2 Hz and 4 Hz stimulation conditions. [Color figure can be viewed in the online issue, which is available at wileyonlinelibrary.com.]

TABLE I. SI and PPC source locations and latencies (mean ± standard deviations across the subjects included in the quantitative analysis)

Source	Location (mm)			Peak latency (ms)
	x (right-left)	y (posterior-anterior)	z (inferior-superior)	
SI	-40 ± 3	7 ± 6	84 ± 5	69 ± 5
PPC	-35 ± 8	-3 ± 10	90 ± 5	98 ± 5

The source locations are expressed in a Cartesian coordinate system defined from external landmarks on the scalp, with x-axis pointing from left to right (through the preauricular points), y-axis from inion to nasion, and z-axis toward the vertex.

and two brain areas under investigation. The peak dipole strengths of SI and PPC responses show progressive attenuation with the serial position of the responses in the train. In addition, the mean data across all subjects indicate a general trend for the evoked PPC responses to exhibit a more pronounced decay of the relative amplitude as compared to SI responses, at each of the two stimulation rates. These qualitative observations were confirmed by three-way repeated measures ANOVA performed on the normalized peak amplitude data (as dependent variable) from each brain area (SI vs. PPC), stimulation rate (2 Hz vs. 4 Hz), and serial position of the pulse within the train. This analysis indicated significant main effects of stimulation rate ($F = 15.8$, $P = 0.005$), brain area ($F = 15.0$, $P = 0.006$), and serial position of the responses ($F = 4.1$, $P = 0.01$). In addition, the interaction between stimulation rate and brain area was found to be significant ($F = 6.3$, $P = 0.04$).

With the exception of the SI evoked response at 2 Hz, the averaged data across subjects (Fig. 6) indicate that the maximal decrement in response amplitude generally occurs with the second response in each train. Further incremental attenuation with the serial position is small for the subsequent pulses, and in several subjects, we observed a slight oscillatory behavior in the response amplitude with the serial position in the train, with responses to the middle stimuli exhibiting a slightly higher amplitude than the response to the second stimulus. This observation that much of the response attenuation occurs between the first and second stimuli in the train is in agreement with previous reports of response suppression at the population level [Angel et al., 1985; Tomberg et al., 1989] or in single upper-layer cortical neurons [Lee and Whitsel, 1992; Lee et al., 1992], whereas a similar oscillatory behavior with the serial position subsequent to the second response in the train was also reported by [Angel et al., 1985], and more recently, in our study using a different type of cutaneous stimulus [Popescu et al., 2010].

DISCUSSION

Previous electrophysiological and neuromagnetic studies using electrical stimulation have provided valuable insights into the cortical somatosensory processing network. However, the advantages of this stimulation modality, that is, easily replicable stimulus parameters and cortical responses, are offset by the fact that the stimulus bypasses the sensory receptors of the skin, entrains undifferentiated afferents, and generates "unnatural" interactions at subcortical and cortical levels. Alternatively, tactile

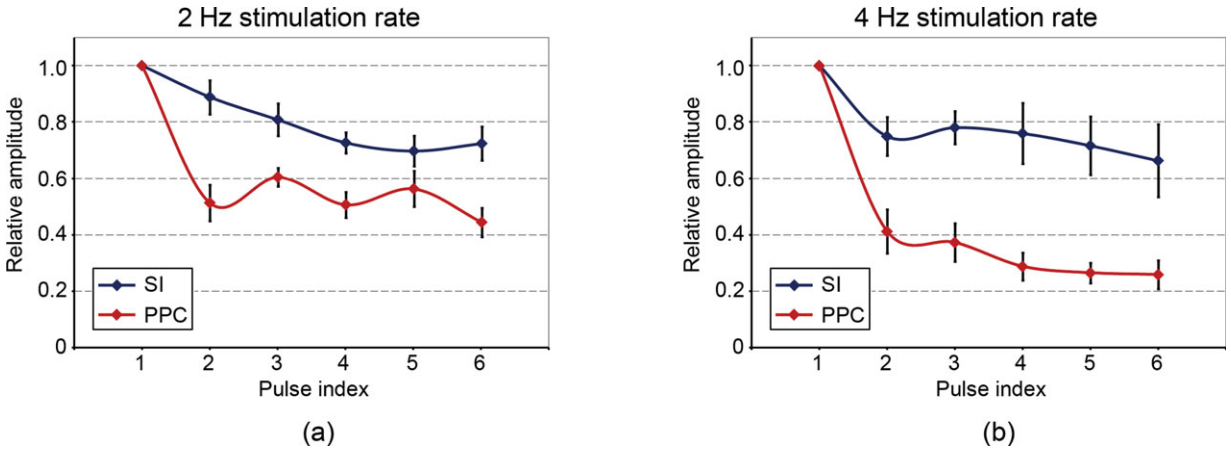

Figure 6.
Adaptation effects in SI and PPC: the mean relative peak amplitude and corresponding standard error of the mean (vertical bars) across subjects are shown for the 2 Hz (**a**) and 4 Hz (**b**) stimulation conditions. The peak amplitudes were normalized with the amplitude of the first response in the train for each subject/condition. The plots were obtained using cubic spline interpolation to display smoothed curves. [Color figure can be viewed in the online issue, which is available at wileyonlinelibrary.com.]

stimuli activate more selectively the sensory pathways that are recruited by somatic inputs during typical sensorimotor behaviors. In this study, we used tactile stimulation paradigms to conduct a comparative analysis of the induced adaptation at multiple levels of the cortical somatosensory network for different stimulation rates.

Cortical somatosensory adaptation inherits inherently some effects of the adaptive changes at lower levels of the ascending sensory pathways. For example, sustained sensory stimulation leads to a temporal desynchronization of the thalamic excitatory inputs and a delay in the arrival of feedforward inhibitory inputs to middle layer cortical neurons in SI, changing their spiking pattern and functional role [Gabernet et al., 2005; Heiss et al., 2008; Wang et al., 2010], In addition to these changes, local cortical adaptation involves also long-lasting lateral interactions between adjacent cortical columns, which may provide a mechanism for the temporal integration of each transient response with an activity trace set by previous stimuli [Lee and Whitsel, 1992; Lee et al., 1992; Whitsel et al., 1989, 1991].

In our study, the dynamics of the neuromagnetic responses likely reflects these adaptation mechanisms occurring at multiple levels of cortical organization. Our results indicate that the adaptation patterns in the somatosensory association areas in PPC exhibit higher sensitivity to stimulus repetition compared with SI. This finding may reflect a cumulative effect of two factors: (1) the inherited effect of adaptation from the lower level (i.e., SI) in a serial SI-PPC processing hierarchy, and (2) the effect of local, dynamically evolving lateral interactions in PPC. The cortical region responsive to our tactile stimulus is located dorso-medial with respect to the SI hand area, which appears to be consistent with the somatosensory association area 5 in PPC [Cavada and Goldman-Rakic, 1989a,b; Kalaska, 1996; Penfield and Jasper, 1954]. Anatomical studies demonstrated a heavy projection from SI to PPC area 5 in rhesus monkey [Jones and Powell, 1970; Pandya and Kuypers, 1969], which indicates that area 5 may be involved in higher order processing of the somatosensory inputs. In addition, it was shown that the neurons in area 5 responding to cutaneous stimuli have larger and more complex receptive fields compared to SI neurons [Kalaska, 1996; Mountcastle, 1995; Murray and Coulter, 1981; Sakata et al., 1973]. Our observation of higher adaptation in the PPC area compared with SI is consistent with previous results showing a trend for higher response suppression and longer lasting activity traces in the association areas with larger neuronal receptive fields compared to primary sensory areas [e.g., auditory studies of Lü et al., 1992]. These findings were interpreted as a potential indication of longer lasting integrative processes in higher order sensory areas and were linked to a functional role that includes maintenance and integration of multiple temporally or spatially dispersed inputs. Although the sensitivity to stimulus repetition was higher in PPC versus SI, the transient responses to each pulse in the train were clearly identifiable at stimulation frequencies of 2 Hz and 4 Hz, indicating that the recovery time in the dorsal association areas is only moderately longer as compared with SI. Along with the short latency delay between the peak activities in SI and PPC, these results appear consistent with the functional role of the somatosensory association areas in PPC in sensorimotor integration, that is, allowing rapid processing and integration of reafferent cutaneous and proprioceptive inputs from unfolding movement, and conveying signals to motor areas [Jones et al., 1978; Kalaska, 1996; Petrides and Pandya, 1984].

In contrast to the areas in PPC, the analysis of adaptive changes in the ventro-lateral somatosensory association areas, that is, SII/PV, has been partially hindered by two factors. First, the bilateral evoked responses reflecting the activity in these areas were not consistently detected across subjects with punctate tactile stimulation, and a relatively large variability in their latency was observed across subjects with identifiable bilateral SEF response. Higher inter-subject variability in the detection of these bilateral late response components for tactile compared to electrical stimulation has been reported previously in several other neuroimaging studies [Forss et al., 1994b; Hari and Forss, 1999; Zhu et al., 2007]. Differences in the stimulation modality (mechanical vs. electrical) is likely to explain such variation, since electrical stimulation recruits many undifferentiated fibers, and therefore increases the likelihood of response detection in regions with large receptive fields. Second, although the bilateral response component to the first stimulus in the train was identifiable in several subjects, the responses to subsequent pulses had very small amplitude, which did not permit their reliable identification and quantification of the adaptive changes in these areas. The results of previous MEG studies on the adaptation profiles in the ventro-lateral somatosensory association areas have been contradictory, in part due to the different stimulation and analysis modalities used in these studies. One study using electrical stimulation of the median nerve at the wrist [Hari et al., 1993] indicated that the amplitude of the SII response depends strongly on the stimulus repetition rate, it does not saturate even at relatively long inter-stimulus intervals of 8 s, and it is difficult to identify in the averaged SEF data for runs with regular ISIs of 0.5 s or shorter. In contrast, another study using electrical stimulation of the fingers [Hamada and Suzuki, 2005] reported that SII responses can be seen in neuromagnetic recordings with ISIs as short as 100 ms and have a recovery lifetime only slightly longer than that in SI. Our results obtained with punctate tactile stimuli applied to the fingers agree with the first report in showing that the bilaterally evoked responses in SII/PV areas, if present, exhibit a rapid suppression following the first pulse in the train, even at 2 Hz stimulation frequency. The longer recovery time in these regions appears compatible with their predominant role in tasks requiring maintenance and integration of sensory inputs over relatively longer temporal scales, such as tactile recognition, learning, and discrimination [Hodzic et al., 2004; Mishkin, 1979;

Murray and Mishkin, 1984; Roland et al., 1998; Servos et al., 2001], and parallels similar observations made in the secondary auditory cortical areas [Lü et al., 1992].

The effectiveness of our neuromagnetic study in characterizing the neuronal adaptation in the dorsal areas of the somatosensory pathway, together with their previously documented role in sensorimotor integration, suggests that such an approach can support future studies of cortical response adaptation in patients with sensorimotor deficits. Existing evidence indicate that these patients exhibit symptoms of "fading sensation" in the presence of sustained somatic inputs [Dannenbaum et al., 2002], which can be potentially related to abnormal patterns of adaptation in the dorsal somatosensory areas. In addition, the methodology and the results of our study can provide a basis for investigating the relationship between neuronal activity and hemodynamic response across multiple cortical regions using multimodal fMRI-MEG studies, which represents an active research area with potential applications in clinical conditions associated with abnormal neurovascular coupling.

ACKNOWLEDGMENTS

We thank Allan Schmitt and Franklin Hunsinger for their help in the acquisition of MRI scans. We thank also the two anonymous reviewers who provided valuable suggestions for improving the manuscript.

REFERENCES

Angel RW, Quick WM, Boylls CC, Weinrich M, Rodnitzky RL (1985): Decrement of somatosensory evoked potentials during repetitive stimulation. Electroencephalogr Clin Neurophysiol 60:335–342.

Caselli RJ (1993): Ventrolateral and dorsomedial somatosensory association cortex damage produces distinct somesthetic syndromes in humans. Neurology 43:762–771.

Cavada C, Goldman-Rakic PS (1989a): Posterior parietal cortex in rhesus monkey. I. Parcellation of areas based on distinctive limbic and sensory corticocortical connections. J Comp Neurol 287:393–421.

Cavada C, Goldman-Rakic PS (1989b): Posterior parietal cortex in rhesus monkey. II. Evidence for segregated corticocortical networks linking sensory and limbic areas with the frontal lobe. J Comp Neurol 287:422–445.

Dannenbaum RM, Michaelsen SM, Desrosiers J, Levin MF (2002): Development and validation of two new sensory tests of the hand for patients with stroke. Clin Rehabil 16:630–639.

Delorme A, Makeig S (2004): EEGLAB: An open source toolbox for analysis of single-trial EEG dynamics including independent component analysis. J Neurosci Methods 134:9–21.

Forss N, Hari R, Salmelin R, Ahonen A, Hämäläinen M, Kajola M, Knuutila J, Simola J (1994a): Activation of the human posterior parietal cortex by median nerve stimulation. Exp Brain Res 99:309–315.

Forss N, Salmelin R, Hari R (1994b): Comparison of somatosensory evoked fields to airpuff and electric stimuli. Electroencephalogr Clin Neurophysiol 92:510–517

Forss N, Hietanen M, Salonen O, Hari R (1999): Modified activation of somatosensory cortical network in patients with right-hemisphere stroke. Brain 122:1889–1899.

Franzén O, Offenloch K (1969): Evoked response correlates of psychophysical magnitude estimates for tactile stimulation in man. Exp Brain Res 8:1–18.

Frostig RD, Xiong Y, Chen-Bee CH, Kvasnák E, Stehberg J (2008): Large-scale organization of rat sensorimotor cortex based on a motif of large activation spreads. J Neurosci 28:13274–13284.

Gabernet L, Jadhav SP, Feldman DE, Carandini M, Scanziani M (2005): Somatosensory integration controlled by dynamic thalamocortical feed-forward inhibition. Neuron 48:315–327.

Gescheider GA, Wright JH (1969): Effects of vibrotactile adaptation on the perception of stimuli of varied intensity. J Exp Psychol 81:449–453.

Goble AK, Hollins M (1993): Vibrotactile adaptation enhances amplitude discrimination. J Acoust Soc Am 93:418–424.

Goble AK, Hollins M (1994): Vibrotactile adaptation enhances frequency discrimination. J Acoust Soc Am 96:771–780.

Hahn JF (1966): Vibrotactile adaptation and recovery measured by two methods. J Exp Psychol 71:655–658.

Hamada Y, Suzuki R (2005): Hand posture modulates cortical finger representation in SII. Neuroimage 25:708–717.

Hamada Y, Otsuka S, Okamoto T, Suzuki R (2002): The profile of the recovery cycle in human primary and secondary somatosensory cortex: A magnetoencephalography study. Clin Neurophysiol 113:1787–1793.

Hari R, Forss N (1999): Magnetoencephalography in the study of human somatosensory cortical processing. Philos Trans R Soc London B Biol Sci 354:1145–1154.

Hari R, Hämäläinen H, Hämäläinen M, Kekoni J, Sams M, Tiihonen J (1990): Separate finger representations at the human second somatosensory cortex. Neuroscience 37:245–249.

Hari R, Karhu J, Hämäläinen M, Knuutila J, Salonen O, Sams M, Vilkman V (1993): Functional organization of the human first and second somatosensory cortices: A neuromagnetic study. Eur J Neurosci 5:724–734.

Hashimoto I, Yoshikawa K, Sasaki M (1990): Latencies of peripheral nerve and cerebral evoked responses to air-puff and electrical stimuli. Muscle Nerve 13:1099–1104.

Heiss JE, Katz Y, Ganmor E, Lampl I (2008): Shift in the balance between excitation and inhibition during sensory adaptation of S1 neurons. J Neurosci 28:13320–13330.

Higley MJ, Contreras D (2006): Balanced excitation and inhibition determine spike timing during frequency adaptation. J Neurosci 26:448–457.

Hironaga N, Ioannides AA (2007): Localization of individual area neuronal activity. Neuroimage 34:1519–1534.

Hodzic A, Veit R, Karim AA, Erb M, Godde B (2004): Improvement and decline in tactile discrimination behavior after cortical plasticity induced by passive tactile coactivation. J Neurosci 24:442–446.

Hsiao S (2008): Central mechanisms of tactile shape perception. Curr Opin Neurobiol 18:418–424.

Hyvärinen A, Oja E (2000): Independent component analysis: Algorithms and applications. Neural Netw 13:411–430.

Jones EG, Powell TPS (1970): An anatomical study of converging sensory pathways within the cerebral cortex of the monkey. Brain 93:793–820.

Jones EG, Coulter JD, Hendry SHC (1978): Intracortical connectivity of architectonic fields in the somatic sensory, motor and parietal cortex of monkeys. J Comp Neurol 181:291–348.

Jones SR, Pritchett DL, Stufflebeam SM, Hämäläinen M, Moore CI (2007): Neural correlates of tactile detection: A combined magnetoencephalography and biophysically based computational modeling study. J Neurosci 27:10751–10764.

Kakigi R, Hoshiyama M, Shimojo M, Naka D, Yamasaki H, Watanabe S, Xiang J, Maeda K, Lam K, Itomi K, Nakamura A (2000): The somatosensory evoked magnetic fields. Prog Neurobiol 61:495–523.

Kalaska JF (1996): Parietal cortex area 5 and visuomotor behavior. Can J Physiol Pharmacol 74:483–498.

Lee CJ, Whitsel BL (1992): Mechanisms underlying somatosensory cortical dynamics. I. In vivo studies. Cereb Cortex 2:81–106.

Lee CJ, Whitsel BL, Tommerdahl M (1992): Mechanisms underlying somatosensory cortical dynamics. II. In vitro studies. Cereb Cortex 2:107–133.

Lü ZL, Williamson SJ, Kaufman L (1992): Behavioral lifetime of human auditory sensory memory predicted by physiological measures. Science 258:1668–1670.

Lundstrom RJ (1986): Responses of mechanoreceptive afferent units in the glabrous skin of the human hand to vibration. Scand J Work Environ Health 12:413–416.

Mauguière F, Merlet I, Forss N, Vanni S, Jousmäki V, Adeleine P, Hari R (1997): Activation of a distributed somatosensory cortical network in the human brain: A dipole modelling study of magnetic fields evoked by median nerve stimulation. I. Location and activation timing of SEF sources. Electroencephalogr Clin Neurophysiol 104:281–289.

McLaughlin DF, Kelly EF (1993): Evoked potentials as indices of adaptation in the somatosensory system in humans: A review and prospectus. Brain Res Brain Res Rev 18:151–206.

Mishkin M (1979): Analogous neural models for tactual and visual learning. Neuropsychologia 17:139–151.

Mountcastle VB (1995): The parietal system and some higher brain functions. Cereb Cortex 5:377–390.

Murray EA, Coulter JD (1981): Supplementary sensory area: The medial parietal cortex in the monkey. In: Woolsey CN, editor. Cortical Sensory Organization, Vol. 1. Multiple Somatic Areas. Clifton, NJ: Humana Press. pp 167–196.

Murray EA, Mishkin M (1984): Relative contributions of SII and area 5 to tactile discrimination in monkeys. Behav Brain Res 11:67–83.

Nangini C, Hlushchuk Y, Hari R (2009): Predicting stimulus-rate sensitivity of human somatosensory fMRI signals with MEG. Hum Brain Mapp 30:1824–1832.

Oldfield RC (1971): The assessment and analysis of handedness: The Edinburgh inventory. Neuropsychologia 9:97–113.

Ou W, Nissilä I, Radhakrishnan H, Boas DA, Hämäläinen MS, Franceschini MA (2009): Study of neurovascular coupling in humans via simultaneous magnetoencephalography and diffuse optical imaging acquisition. Neuroimage 46:624–632.

Pandya DN, Kuypers HG (1969): Cortico-cortical connections in the rhesus monkey. Brain Res 13:13–36.

Pascual-Marqui RD (2002): Standardized low-resolution brain electromagnetic tomography (sLORETA): Technical details. Methods Find Exp Clin Pharmacol 24:5–12.

Penfield W, Jasper H (1954): Epilepsy and the Functional Anatomy of the Human Brain. Boston: Little, Brown and Company.

Petrides M, Pandya DN (1984): Projections to the frontal cortex from the posterior parietal region in the rhesus monkey. J Comp Neurol 228:105–116.

Pons TP, Garraghty PE, Mishkin M (1992): Serial and parallel processing of tactual information in somatosensory cortex of rhesus monkeys. J Neurophysiol 68:518–527.

Popescu M, Barlow S, Popescu EA, Estep ME, Venkatesan L, Auer ET, Brooks WM (2010): Cutaneous stimulation of the digits and lips evokes responses with different adaptation patterns in primary somatosensory cortex. Neuroimage 52:1477–1486.

Pratt H, Politoske D, Starr A (1980): Mechanically and electrically evoked somatosensory potentials in humans: Effects of stimulus presentation rate. Electroencephalogr Clin Neurophysiol 49:240–249.

Renvall H, Lehtonen R, Hari R (2005): Abnormal response recovery in the right somatosensory cortex of dyslexic adults. Cereb Cortex 15:507–513.

Roland PE, O'Sullivan B, Kawashima R (1998): Shape and roughness activate different somatosensory areas in the human brain. Proc Natl Acad Sci USA 95:3295–3300.

Sakata H, Takaoka Y, Kawarasaki A, Shibutani H (1973): Somatosensory properties of neurons in the superior parietal cortex (area 5) of the rhesus monkey. Brain Res 64:85–102.

Servos P, Lederman S, Wilson D, Gati J (2001): fMRI-derived cortical maps for haptic shape, texture, and hardness. Brain Res Cogn Brain Res 12:307–313.

Schnitzler A, Volkmann J, Enck P, Frieling T, Witte OW, Freund HJ (1999): Different cortical organization of visceral and somatic sensation in humans. Eur J Neurosci 11:305–315.

Tomberg C, Desmedt JE, Ozaki I, Nguyen TH, Chalklin V (1989): Mapping somatosensory evoked potentials to finger stimulation at intervals of 450 to 4000 msec and the issue of habituation when assessing early cognitive components. Electroencephalogr Clin Neurophysiol 74:347–358.

Tommerdahl MA, Whitsel BL (1996): Optical imaging of intrinsic signals in somatosensory cortex. In: Franzen O, Johansson R, Terenius L, editors. Somesthesis and the Neurobiology of the Somatosensory Cortex. Basel, Switzerland: Birkhäuser-Verlag. pp 369–384.

Tommerdahl MA, Hester KD, Felix ER, Hollins M, Favorov OV, Quibrera PM, Whitsel BL (2005): Human vibrotactile frequency discriminative capacity after adaptation to 25 Hz or 200 Hz stimulation. Brain Res 1057:1–9.

Venkatesan L, Barlow S, Popescu M, Popescu A, Auer ET (2010): TAC-Cell inputs to human hand and lip induce short-term adaptation of the primary somatosensory cortex. Brain Res 1348:63–70.

Vigário R, Särelä J, Jousmäki V, Hämäläinen M, Oja E (2000): Independent component approach to the analysis of EEG and MEG recordings. IEEE Trans Biomed Eng 47:589–593.

Wang Q, Webber RM, Stanley GB (2010): Thalamic synchrony and the adaptive gating of information flow to cortex. Nat Neurosci 13:1534–1541.

Whitsel BL, Favorov O, Tommerdahl MA, Diamond M, Juliano S, Kelly DG (1989): Dynamic processes governing the somatosensory cortical response to natural stimulation. In: Lund JS, editor. Sensory Processing in the Mammalian Brain. New York: Oxford University Press. pp 84–116.

Whitsel BL, Favorov O, Kelly DG, Tommerdahl MA (1991): Mechanisms of dynamic peri- and intra-columnar interactions in somatosensory cortex: Stimulus specific contrast enhancement by NMDA receptor activation. In: Franzen O, Westman J, editors. Information Processing in Somatosensory System. London: Macmillan Press. pp 353–369.

Willis WD Jr, Coggeshall RE. 1991. Sensory Mechanisms of the Spinal Cord. New York: Plenum.

Young JP, Herath P, Eickhoff S, Choi J, Grefkes C, Zilles K, Roland PE (2004): Somatotopy and attentional modulation of the human parietal and opercular regions. J Neurosci 24:5391–5399.

Zhu Z, Disbrow EA, Zumer JM, McGonigle DJ, Nagarajan SS (2007): Spatiotemporal integration of tactile information in human somatosensory cortex. BMC Neurosci 8:8–21.